ELSEVIER

Psychiatry Research: Neuroimaging Section 90 (1999) 113–123

PSYCHIATRY RESEARCH
NEUROIMAGING

MRI volume of the amygdala: a reliable method allowing separation from the hippocampal formation

Antonio Convit[a,b,*], Pauline McHugh[a], Oliver T. Wolf[a], Mony J. de Leon[a,b], Maciek Bobinski[c], Susan De Santi[a], Alexandra Roche[a], Wai Tsui[a,b]

[a] *Department of Psychiatry, New York University School of Medicine, Aging and Dementia Research Center, Neuroimaging Laboratory, HN-314, New York University School of Medicine, 560 First Avenue, New York, NY 10016, USA*
[b] *Nathan Kline Institute for Psychiatric Research, Orangeburg, NY, USA*
[c] *Institute for Brain Research, Staten Island, NY, USA*

Received 2 November 1998; received in revised form 2 February 1999; accepted 4 February 1999

Abstract

Studies of MRI-derived volume of the amygdala have been mostly performed on coronal sections where its boundaries with the hippocampus and the entorhinal cortex are indistinct. To date, all reports of in vivo amygdala volume have consistently overestimated the size of the structure. We have developed a method for the MRI-based in vivo measurement of the amygdala volume which allows a better separation of the amygdala from the adjoining hippocampal formation. In nine normal volunteers we obtained three-dimensional spoiled gradient recalled acquisition, 1.3-mm thick, T1 weighted sagittal MR images and created electronically linked reformatted images in the coronal and axial planes. On the original sagittal and the reformatted axial planes, where it is more readily apparent, we delineated the boundaries between the amygdala and the hippocampus and the amygdala and the hippocampo–amygdala transition area, respectively. We then projected those markings onto the coronal plane, where the other boundaries of the amygdala are more easily seen. Using these markings as a guide and utilizing extra-amygdalar coronal landmarks for the anterior end, we outlined the whole amygdala on the coronal plane and determined its volume. We observed that 45% of the coronal slices that contained amygdala also contained some hippocampus. The amygdala measurement had high test–retest reliability, with an intra-class correlation coefficient (r_{ICC}) of 0.99 for the total volume and an r_{ICC} of 0.93 for the measurement at the level of the individual slice. The average amygdala volume was 1.05 ± 0.17 cm^3 on the right and 1.14 ± 0.15 cm^3 on the left. Our amygdala volumes are in agreement with those reported in postmortem studies, which provides the reported method with face validity.

* Corresponding author. Tel.: +1 212 2637565; fax: +1 212 2636991; e-mail: antonio.convit@mcadr.med.nyu.edu

PII: S0925-4927(99)00007-4

The ability to reliably and validly measure the amygdala in vivo may facilitate the investigation of psychiatric disorders, such as PTSD, anxiety disorders, and schizophrenia, which are presumed to have amygdala dysfunction and pathology.

Keywords: Amygdala; Hippocampus; Magnetic resonance imaging; Volume measurement; Method

1. Introduction

The amygdala has been documented to have an important role in fear, smell, rage and emotional memory (Aggleton, 1992; LeDoux, 1995; McGaugh and Cahill, 1997). It is therefore possible that the amygdala may have an important role in psychiatric conditions such as post-traumatic stress disorder (PTSD), anxiety disorders, and schizophrenia. The amygdala is positioned in the dorsomedial portion of the temporal lobe, in close proximity to the medial temporal lobe regions, such as the hippocampal formation (hippocampus proper, subiculum, and entorhinal cortex) and to other gray-matter structures, such as the claustrum and tail of the caudate. All of these temporal lobe structures have similar MRI signal intensities, a fact which obscures their shared boundaries and has led to difficulties in accurately measuring the size of the amygdala in vivo using MRI. In fact, early studies did not attempt to separate the amygdala and the hippocampus but measured them together, thereby creating a so called amygdala–hippocampal complex (DeLisi et al., 1988; Shenton et al., 1992; Bogerts et al., 1993; Buchanan et al., 1993). Many in vivo amygdala measurements have been carried out in neuropsychiatric conditions, such as schizophrenia, temporal lobe epilepsy, and Alzheimer's disease (e.g. Tsuchiya and Kosaka, 1990; Cendes et al., 1993a,b; Cuenod et al., 1993; Lehéricy et al., 1994; Watson et al., 1997; Lawrie and Abukmeil, 1998). There is considerable variability across studies with overestimates of the volume generally reported. Moreover, existing amygdala measurement methods have resulted in large differences across studies even for normal brain, resulting, on average, in volumes 1.5–3 times those reported in the neuropathology literature.

MRI studies of the amygdala have generally utilized the coronal orientation for the volume determinations. Several approaches to measuring the amygdala volume on coronal orientation have been reported and salient examples of each are presented in Table 1. Some investigators dealt with the indistinct boundary between the amygdala and the hippocampal formation on coronal view by measuring a fixed number of slices where the amygdala is clearly visible. However, this resulted in the exclusion of an undetermined amount of amygdaloid tissue (see Table 1, row 1). Other groups attempted to measure the entire amygdala, but again only utilized coronal anatomy to determine the boundaries, which likely led to errors in the determination of the amygdala–hippocampal boundary (Table 1, row 2). Several research groups have attempted to standardize the coronal measurements by utilizing other brain anatomical landmarks as a reference to determine beginning and/or end slices or for in-plane amygdala boundaries (Table 1, row 3). Finally, some investigators have combined the use of extra-amygdalar landmarks with the use of other reformatted planes to cross-check the markings made on the coronal plane (Table 1, row 4). There is a single report in the literature where amygdala volume measurements were carried out on an axial orientation utilizing the other two orthogonal planes to cross-check their markings (Honeycutt et al., 1998). These investigators reported high reproducibility for their method, but did not report on the actual amygdala volumes obtained.

The methods utilized to date have resulted in large variability of the reported volumes. The volumes reported range from 1.3 cm^3 in studies sampling a fraction of the total amygdala to 3.4 cm^3 in studies measuring the whole amygdala.

Table 1
A comparison of methods developed for measuring amygdala volume

Method used	Reference examples	Amygdala volume	Slice thickness	Angle perpendicular to	Reformatted	Reliability reported
1. Restricted amount of slices	Barta et al., 1990	1.45 cm^3 (R) 1.54 cm^3 (L)	3 mm	AC–PC	No	Yes
	Rossi et al., 1994	1.31 cm^3 (R) 1.25 cm^3 (L)	5 mm	AC–PC	No	Yes
2. Boundaries estimated from coronal slices	Bartzokis et al., 1993	Values not reported	3 mm	LAHC	No	Yes
	Soininen et al., 1994	1.69 cm^3 (R) 1.85 cm^3 (L)	1 mm	LAHC	No	Yes
	Laakso et al., 1995	2.16 cm^3 (R) 2.35 cm^3 (L)	1.5–2 mm	LAHC	No	Previously published
3. Estimated boundaries on coronal and external landmarks	Bogerts et al., 1993	1.91 cm^3 (R) 1.61 cm^3 (L)	3.1 mm	Not reported	No	Yes
	Watson et al., 1992	3.44 cm^3 (R) 3.34 cm^3 (L)	3 mm	LLSC	No	Yes
	Lehéricy et al., 1994	2.24 cm^3 (R) 2.16 cm^3 (L)	5 mm	LAHC	No	Yes
	Jack et al., 1997	Not reported	1.6 mm	LAHC	Yes	Not reported
	Krasuki et al., 1998	1.97 cm^3 (R + L)/2	5 mm	LSF	No	Yes
4. Using multiple planes and external landmarks	Kates et al., 1997	Values not reported	1.5 mm	AC-PC and/or LAHC	Yes	Yes
	Sheline et al., 1998 [a]	1.8 cm^3 (R) 1.8 cm^3 (L)	0.5 mm	AC-PC	Yes	Yes

Notes. AHC, anterior amygdala–hippocampal complex; AC–PC, anterior commissure–posterior commissure; LAHC, long axis of the hippocampus; LLSC, left lateral sulcus; LSF, left sylvian fissure.
[a] This report used stereological techniques.

Several postmortem studies have reported the *total* amygdala volumes to be between 1.1 and 1.6 cm^3 (Herzog and Kemper, 1980; Bogerts et al., 1985; Heckers et al., 1990; Scott et al., 1991), thereby providing a benchmark to evaluate the validity of MRI-derived volume estimates. Although it is difficult to assess the face validity of studies that measure only a limited portion of the amygdala, it is clear that most studies measuring the whole structure overestimate the volume by as much as 200%.

We have developed a strategy to obtain reliable measures of the amygdala on MRI such that the entire structure is measured without the inclusion of adjacent structures and with minimal reliance on extra-amygdala landmarks. This method, which uses information about the boundaries from three orthogonal planes, enables the operator to identify and exclude hippocampus, hippocampal–amygdala transition area, and entorhinal cortex from the amygdala measurements. In this communication we will describe this in vivo MRI

method, provide test–retest reliability for the measurements, report the volumes on a small group of normal individuals, and contrast our findings with those reported in the neuropathological literature.

2. Methods

2.1. Subjects

Nine Caucasian male normal volunteers between the ages of 30 and 52 (mean age 37.4 ± 8.4), with between 16 and 22 years of formal education, participated in the study. The presence of any significant psychiatric condition was excluded using the Quick Diagnostic Interview Schedule (Robins et al., 1981). Moreover, subjects were thoroughly evaluated to ensure they were free of significant neurologic, metabolic, or cardiovascular disease. For the assessment of the reliability of the measurement method, a separate group of five young schizophrenic males, who were part of a separate study that had used identical image acquisition parameters, was utilized. All subjects gave written informed consent.

2.2. MRI evaluations

Subjects were scanned on a 1.5-T GE Advantage MR system. We obtained three sequences with a total scan time of approximately 25 min: a sagittal three-dimensional spoiled gradient recalled acquisition (SPGR) for the volume measurements and axially acquired fast spin echo proton density and T2-weighted images to exclude gross brain pathology. The SPGR images were obtained using the following parameters: TR 35/TE 9 ms, 60° flip angle, 1.1 mm slice thickness with no gap, a 24-cm FOV, a 256 × 192 matrix, and one excitation, for a total of 124 slices. The proton density and T2-weighted images, which were utilized to rule out gross brain abnormalities, had the following parameters: TR = 7000 and TE = 100 ms, FOV = 20 cm, 256 × 256 matrix, one excitation, with contiguous 3-mm slices with no gaps.

2.3. Image standardization and image analysis

Anatomical measurements were performed on a graphic workstation (Sun Microsystems Sparc; UNIX operating system) using the Multimodal Image Data Analysis System (MIDAS) (Tsui, 1995). MIDAS has a reformatting routine which allowed us to 'cut' an image at any level to produce a multi-slice orthogonal image. This reformatting routine was used to create standardized coronal images from the sagittal image set that approximated the pathological-angle coronal images typically used in postmortem studies. This coronal image set was created from the SPGR sagittal images utilizing the image in the mid-sagittal plane as follows: (1) the point where the tentorium cerebelli intercepts the dura in the posterior occipital region was identified; (2) a line joining this point to the inferior surface of the orbitofrontal cortex was drawn; and (3) the pathological angle coronal plane was defined as the plane perpendicular to this line. To create the reformatted pathological angle coronal images, we used a slice thickness of 0.87 mm to coincide with the width of the pixel in the original sagittal image. Reformatting to the pathological plane enabled us to use standard neuroanatomical atlases (Roberts and Hanaway, 1970; Duvernoy, 1988) as a guide.

2.3.1. Separation of amygdala from hippocampus and from hippocampal–amygdala transition area

The amygdala is an almond-shaped structure, which is situated anterior and partly superior to the tip of the temporal horn of the lateral ventricle. On the coronal plane the boundary between hippocampus and amygdala is often indistinct. However, this boundary is more readily identified on the sagittal plane. In the sagittal plane the anterior boundary of the hippocampus is very clear. Using MIDAS, we marked this anterior hippocampal boundary on the sagittal images. Fig. 1 depicts the results of this process. Panels A–D show the operator-determined markings of the anterior hippocampal boundary on a few of the sagittal slices going from lateral (A) to medial

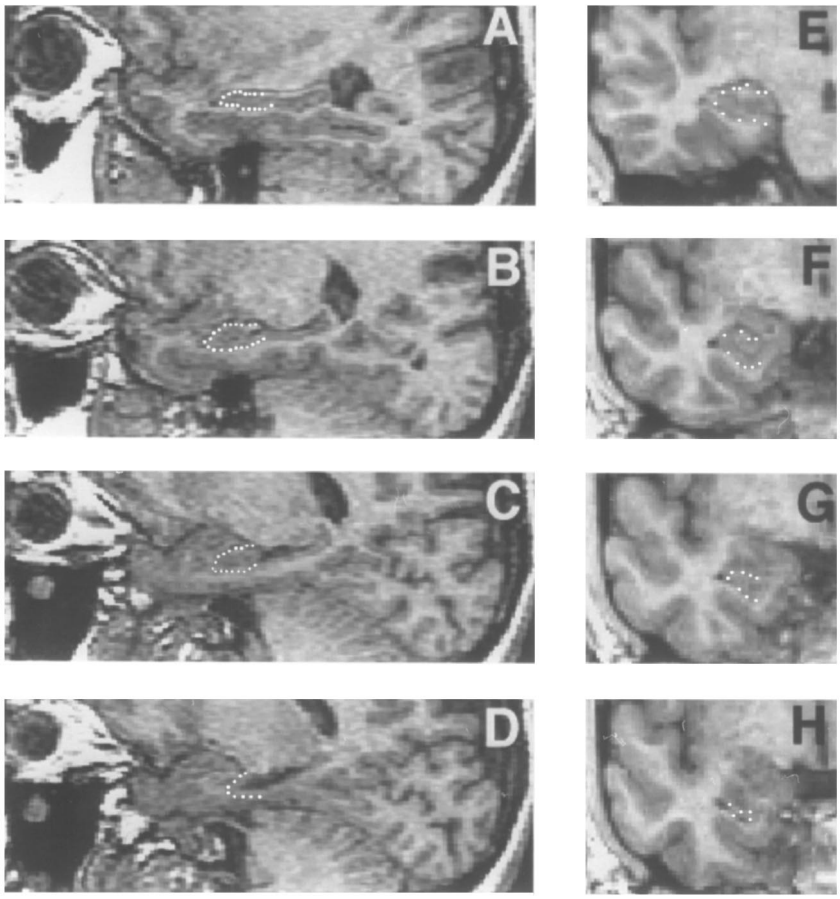

Fig. 1. Separation of the hippocampus from the amygdala. The four left panels depict representative sagittal slices going from lateral (A, top) to medial (D, bottom) on which the anterior aspects of the hippocampus are outlined (white dots). The set of four panels on the right depict four representative coronal slices showing the markings retained from the reformatting of the sagittal images. Each of the sagittal images where the anterior end of the hippocampus was outlined will contribute one or two dots to any one coronal slice reformatted from the sagittal set. The top right panel (E) is at the level of the uncus of the hippocampus, where no amygdala appears. The other three right panels represent successively more anterior coronal sections, with the anterior-most (H, bottom) showing only a sliver of the hippocampus–subicular complex with a large amygdala above.

(D). These anterior hippocampal markings are retained when creating the reformatted pathological angle coronal images as described above. Thus, the separation more easily seen on the sagittal orientation was projected onto the coronal view. This procedure also established the superior boundary of the hippocampus, which corresponds to the inferior border of the amygdala in the coronal plane. Panels E–H display those markings after they have been electronically reformatted to the coronal pathological plane, going from posterior (E) to anterior (H). Please note that the sagittal and coronal images presented in Fig. 1 are orthogonal; only one or two dots seen on a coronal image originate from any one sagittal slice.

At the posterior end of the amygdala, the rounded cortical nucleus of the amygdala transitions to a thin strip of gray matter, which in turn connects to the subiculum of the hippocampus. This strip of gray matter forms an anatomical structure known as the hippocampal–amygdala

transitional area (HATA) (Rosene and Van Hoesen, 1987). This transitional area has distinct cellular components and connections and is not considered to be either part of the hippocampus or the amygdala. On the pathological angle coronal orientation, the HATA appears at the level of the mamillary bodies, and coincides with the posterior pole of the amygdala. In order to reliably separate the HATA from the amygdala and from the hippocampus, we outlined the HATA on the axial plane, where its boundaries are more readily identified, and then projected those markings to the coronal orientation in order to facilitate measurements. Fig. 2 illustrates this process. Panel A represents an axial image (orthogonal to the pathological coronal plane) through the mammillary bodies (3). The HATA has been outlined and separated from the hippocampus (2) and amygdala (1). Those outlines are then reformatted onto the coronal image and are displayed on panel B, where they are seen end on, as horizontal lines, representing the outlines at different axial levels.

2.3.2. Demarcation of the other amygdalar boundaries

After the amygdalar–hippocampal and the HATA–amygdalar boundaries were marked, forming the posterior and anterio-inferior border of the amygdala, the remaining amygdala boundaries were drawn in the coronal plane in a standardized way. Moreover, MIDAS allows, at a pixel-by-pixel level, comparison of any boundary on the coronal plane with its orthogonal counterpart (i.e. sagittal or axial). Fig. 3 depicts the different structures, which are indicated by the numbers in parentheses, utilized for those boundary determinations. Panel A represents a

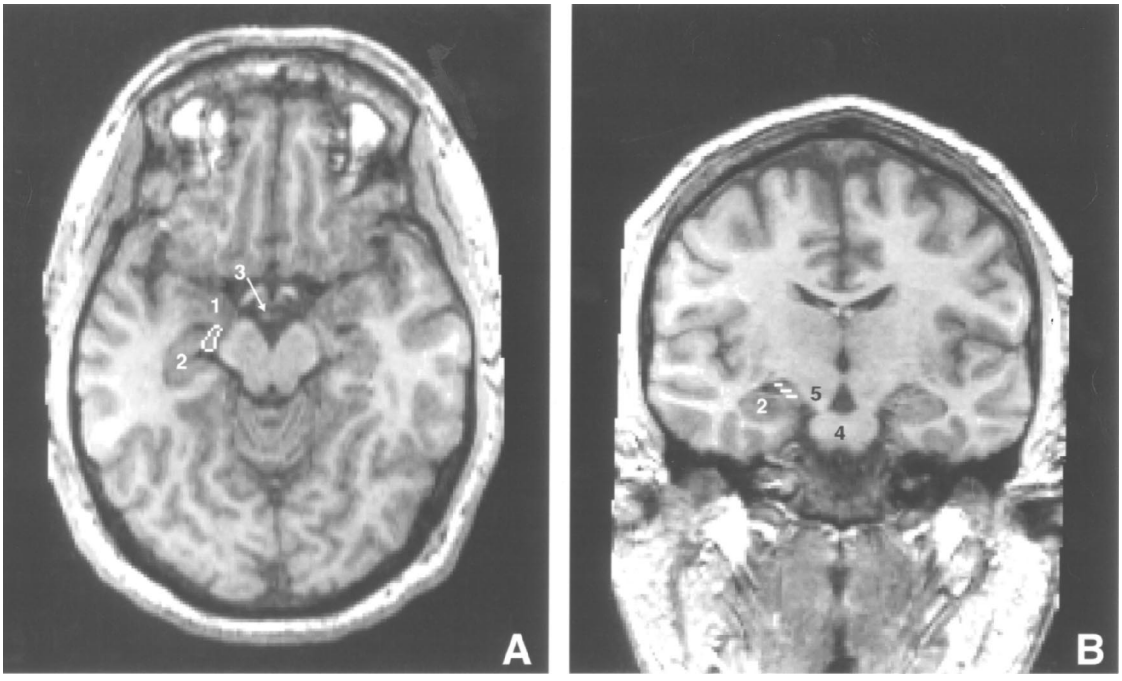

Fig. 2. The axial plane shows the hippocampal–amygdala transition area (HATA; Panel A, outlined in white) which links the posterior pole of the amygdala with the anterior hippocampus. The HATA is readily seen on a horizontal (axial) plane, orthogonal to the pathological coronal orientation, running through the mammillary bodies. The HATA markings (seen in Panel A) were transposed to the coronal plane (Panel B), where they appear as horizontal white lines. Numbers refer to: 1, Amygdala; 2, Hippocampus; 3, Mammillary bodies; 4, Pons; 5, Cerebral peduncles.

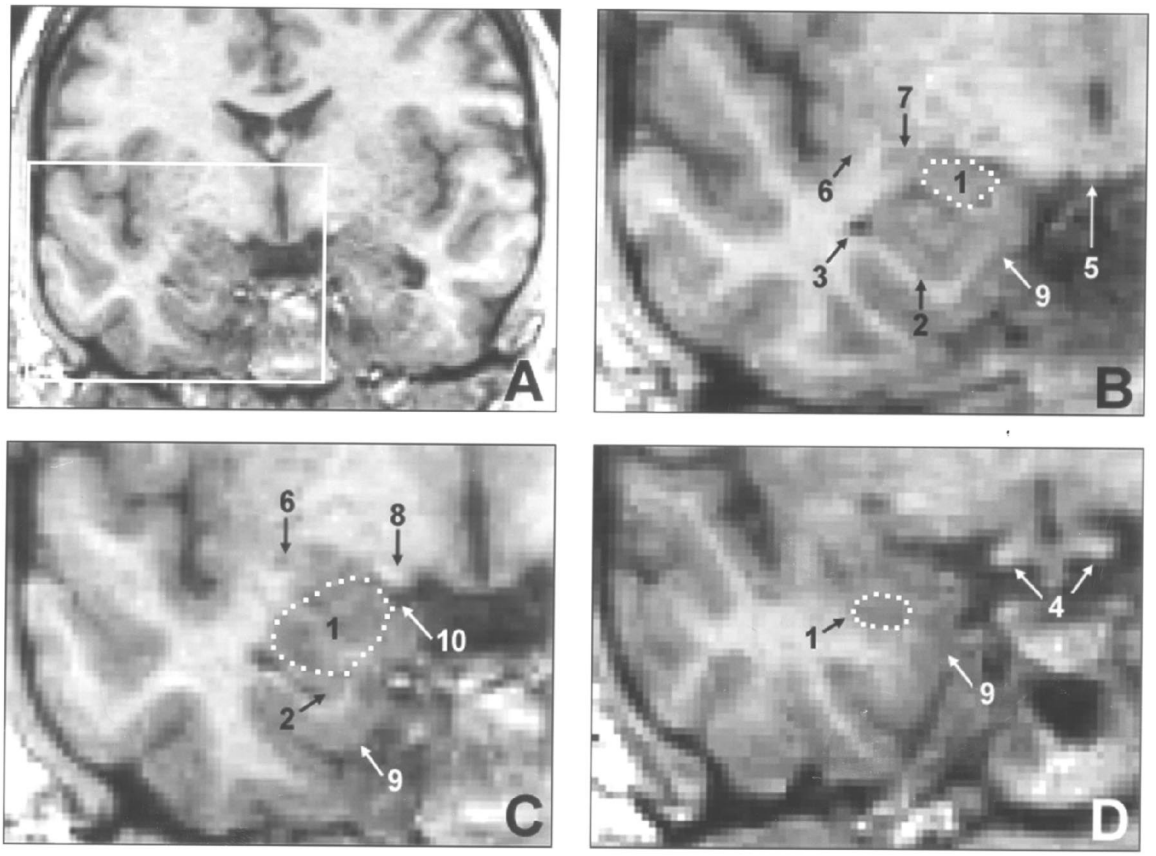

Fig. 3. Landmarks used to identify amygdala boundaries. Panel A shows a coronal section with the temporal right lobe highlighted by the white box. Panels B–D show the magnified right temporal lobe going from posterior (B) to anterior (D) with the amygdala outlined with white dots to allow better visualization of the underlying anatomy. Panel B depicts a section showing the posterior amygdala and its relationship to the hippocampus (below) and the tail of the caudate (laterally). Panel C shows a slice through the middle of the amygdala. Panel D shows the anterior-most aspect of the amygdala, at the level where the optic tract emerges from the cerebri to form the optic chiasm. Numbers in the figure refer to: 1, Amygdala; 2, Hippocampus; 3, Temporal horn of the lateral ventricle; 4, posterior aspect of optic chiasm; 5, Mammillary bodies; 6, Claustrum; 7, Tail of the caudate; 8, Optic tract; 9, Entorhinal cortex; 10, Sulcus semiannularis.

full coronal slice highlighting the temporal lobe (inside the white box), which is then magnified going from posterior (B) to anterior (D).

- The medial border of the amygdala (1) is a thin strip of parahippocampal white matter called the angular bundle, which separates it from the entorhinal cortex (9). This white matter strip becomes indistinct as the slices proceed anteriorly. This white matter tract is oriented obliquely and runs parallel to the entorhinal cortex to the sulcus semiannularis (10 in Panel C), which separates the semilunar gyrus from the ambiens gyrus (entorhinal cortex). On the coronal orientation the sulcus semiannularis is inferior to the optic tract (8). The ambiens gyrus in predominantly made up of entorhinal cortex and the semilunar gyrus contains the cortical nucleus of the amygdala anteriorly.
- The claustrum (6) and tail of the caudate (7) are identified and tracked from slice to slice. The tail of the caudate is present in sections at the level of the mammillary bodies (5). The

claustrum and tail of the caudate are separated from the amygdala gray by thin strips of white matter. The identification of this demarcation, in some cases, can be made easier by referring to the sagittal view, where it may also be visualized. These thin strips of white matter represent the superio-lateral borders of the amygdala. The inferior boundary is the hippocampus (2). As a rule of thumb, the anterior limit of the subiculum is the first hippocampal subdivision to appear ventral to the amygdala, about 6 mm behind the anterior limit of the amygdala. The inferio-lateral border of the amygdala is the temporal lobe white matter and the extension of the temporal horn (3).

- The superio-medial border of the amygdala is demarcated by where the semilunar gyrus, which contains part of the cortical nucleus of the amygdala, comes in contact with the overlying cerebrospinal fluid (CSF).
- The anterior pole of the amygdala is found approximately 7 mm posterior to the fronto–temporal junction and approximately 5 mm behind the anterior limit of the entorhinal cortex (Amaral and Insausti, 1990). The anterior amygdaloid area (AAA, and represented by 1 in panel D) is difficult to distinguish even on histological slides. There is very little white matter between the thick cortical ribbon and the AAA, making it difficult to separate the AAA from the pariamygdaloid cortex dorsally and from the entorhinal cortex more ventromedially. To overcome this problem, we defined the anterior amygdala boundary as that level corresponding to the section immediately posterior to the section where the optic chiasm (4 in panel D) first appears as a continuous structure.

2.3.3. Calculation of the amygdala volume

After outlining the amygdala on all coronal slices where the structure appears, the volume of the structure was calculated by summing the ROI pixel counts across coronal slices and then multiplying by the pixel volume.

2.3.4. Reliability of the measurement

Following the techniques and rules outlined above, the outlining of the amygdala was done by consensus of two raters (AC and PM). In order to assess the reproducibility of our method, measurements were also performed on the right amygdala for a group of five young schizophrenic patients, totaling 58 drawings at the level of the individual slice. The drawings were repeated, blind to the original drawings, 6 weeks apart. The reliability of the measurement across two independent measurements, both at the level of the total right amygdala volume ($N = 5$) and at the level of the individual slice measurements ($N = 58$), was then assessed using the intraclass correlation coefficient (r_{ICC}).

2.3.5. Measurement of the intracranial volume

In order to place our amygdala volume measurements in the context of overall intracranial volume, we measured the cerebral vault by outlining the supratentorial dural margins. Starting at the mid-sagittal slice, and then every fifth sagittal image in either direction, at 6-mm intervals, we outlined the cerebral vault by following the dural and tentorial margins. The total volume was then calculated.

3. Results

We obtained excellent test–retest reliability. For the whole right amygdala volume ($N = 5$), the r_{ICC} was 0.99, and for measurement at the level of the individual slices that made up those five volumes ($N = 58$), the r_{ICC} was 0.93.

The amygdala and intracranial volumes are presented in Table 2. The left amygdala tended to

Table 2
Head and amygdala volumes in normal subjects

Structure	Mean ± S.D.
Volume of left amygdala	1.14 ± 0.17 cm^3
Volume of right amygdala	1.05 ± 0.15 cm^3
Volume of cerebral vault	1284.9 ± 78.8 cm^3
Ratio of left amygdala/cerebral vault	$(0.89 \pm 0.11) \times 10^{-3}$
Ratio of right amygdala/cerebral vault	$(0.82 \pm 0.09) \times 10^{-3}$

be present on more slices (15.4 ± 1.13 vs. 14.1 ± 1.83; $t(8) = 2.14$, $P = 0.06$) than the right and was non-significantly larger (1.14 ± 0.17 cm^3 vs. 1.05 ± 0.15 cm^3). On average the amygdala and the hippocampus overlapped in 8.22 ± 1.39 slices for the left side and 7.56 ± 2.07 slices for the right side. The cerebral vault was 1284.9 ± 78.8 cm^3. The relationship between amygdala volume and intracranial volume, although sizable, did not reach significance, probably due to the small sample size (left, $r = 0.60$, $P = 0.08$; right, $r = 0.59$, $P = 0.09$).

4. Discussion

The amygdala has been associated with a number of important brain functions, and volume alterations are known to occur at postmortem for several pathological conditions (Aggleton, 1992). Inconsistencies in the in vivo measurement of the amygdala have hindered research in those conditions. The development of a valid and reliable MRI measurement method may serve to direct further research towards amygdala change and its relationship to psychiatric disease.

Most reported methods to measure the volume of the amygdala have relied on external brain landmarks to make decisions about boundaries and/or to select slices for measurement. The selection of equivalent slices across cases, when using external brain landmarks, is dependent on the reproducibility of the coronal plane used, the slice thickness, and the anatomical uniformity of the individuals being assessed. Variability in the angle of coronal cut will lead to variability in the appearance of the external landmarks, which will result in different slices selected for measurement across cases. This will lead to added noise in the amygdala volume determination. As a case in point, when the angle of coronal section was modified by 10 degrees, which can happen easily unless a strict protocol is followed, the anterio–posterior position of the mammillary bodies, structures commonly used to determine the posterior end of the amygdala (e.g. Bogerts et al., 1993), shifted by 2–3 mm when using 1 mm-thick slices. This source of variability can be kept to a minimum by either reformatting images (as we have done) or tightly controlling the setup prior to image acquisition.

We have illustrated the method reported here by demonstrating that the amygdala of normal individuals measures approximately 1.14 ± 0.17 cm^3 (left) and 1.05 ± 0.15 cm^3 (right). There are clusters of amygdala cells in the anterior amygdaloid area that were not included in our measurements. That may explain why our in vivo volume measurements were slightly smaller than those reported for normals in the neuropathology literature. After correcting for fixation-related shrinkage, neuropathological studies report amygdala volumes between 1.10 cm^3 and 1.60 cm^3 (Herzog and Kemper, 1980; Bogerts et al., 1985; Heckers et al., 1990; Scott et al., 1991). Two of those studies report standard deviations (S.D.) similar to those in our data (0.09–0.14) (Heckers et al., 1990; Scott et al., 1991). However, a third study reported an unusually large S.D. (0.78), which appears to be caused by one outlier (Bogerts et al., 1985). The fourth article does not report any description of the variance of the measurement (Herzog and Kemper, 1980). In contrast, other in vivo neuroimaging studies appear to consistently overestimate the amygdala volume. Previous studies, when measuring the whole structure, have reported volumes up to three times those reported at postmortem and about the size of those at postmortem when only measuring part of the structure. Those other in vivo MRI studies probably included an undetermined volume of hippocampal tissue. One recent study, which carried out the measurements on the axial orientation, did not report the result of their volume estimations (Honeycutt et al., 1998).

We found that the left amygdala was somewhat larger than the right, which is in agreement with two previous studies (Soininen et al., 1994; Laakso et al., 1995). Other reports have failed to either find a difference (Lehéricy et al., 1994; Filipek et al., 1997) or found the right amygdala to be larger (Filipek et al., 1994; Watson et al., 1992; Krasuki et al., 1998). Aside from issues of lateralization, the volume of the amygdala has a fair degree of

association with the volume of the cerebral vault ($r = 0.6$) and consequently, in clinical studies where different clinical groups are contrasted, individual variability in cerebral vault size should be taken into account (Mathalon et al., 1993).

The novel method described in this communication allows for more accurate measurement of the amygdala by using boundaries determined from multi-planar views. It is worth mentioning that, just as the hippocampus and other gray matter structures have been sources of error for amygdala measurements, so has the amygdala been a source of error for measurements of hippocampal formation structures. Therefore this method will be of use not only in studies involving the amygdala, but in studies of other medial temporal lobe structures.

We have developed a reliable method that addresses some of the weaknesses in prior reports. Our method has the following advantages: (1) it measures the amygdala in its entirety; (b) it does not rely on external anatomical landmarks to establish boundaries (the only exception to this being at the anterior amygdaloid area); (c) it specifically excludes the adjacent hippocampus, entorhinal cortex, and hippocampal–amygdala transition area from the measurement; and (d) it generates amygdala volumes that are very close to the results of histopathological studies. In our experience, differentiating the amygdala from the hippocampus is crucial, given that both structures were present in about half of the slices where the amygdala was present in the coronal orientation. Future studies utilizing MRIs of postmortem brains, which can then be sectioned and studied histologically, will offer the ultimate validation for the method described here.

Acknowledgements

This work was, in part, supported by grants from the National Institute on Aging P30 AG08051, RO1 AG12101, RO1 AG13616, Deutsche Forschungsgesellschaft WO 733/1-1, and the New York State Office of Mental Health. The authors wish to thank Adam Scherer for his valuable assistance with the figures.

References

Aggleton, J.P., 1992. The Amygdala: Neurobiological Aspects of Emotion, Memory and Mental Dysfunction. Wiley-Liss, New York.

Amaral, D.G., Insausti, R., 1990. Hippocampal formation. In: Paxinos, G. (Ed.), The Human Nervous System. Academic Press, San Diego, pp. 711–755

Barta, P.E., Pearlson, G.D., Powers, R.E., Richards, S.S., Tune, L.E., 1990. Auditory hallucinations and smaller superior temporal gyral volume in schizophrenia. American Journal of Psychiatry 147, 1457–1462.

Bartzokis, G., Mintz, J., Marx, P., Osborn, D., Gutkind, D., Chiang, F., Phelan, C.K., Marder, S.R., 1993. Reliability of in vivo volume measures of hippocampus and other brain structures using MRI. Magnetic Resonance Imaging 11, 993–1006.

Bogerts, B., Meertz, M., Schoenfeld-Bausch, R., 1985. Basal ganglia and limbic system pathology in schizophrenia. Archives of General Psychiatry 42, 784–791.

Bogerts, B., Lieberman, A., Ashtari, M., Bilder, R.M., Degreef, G., Lerner, G., Johns, C., Masiar, S., 1993. Hippocampus–amygdala volumes and psychopathology in chronic schizophrenia. Biological Psychiatry 33, 236–246.

Buchanan, R.W., Breier, A., Kirkpatrick, B., Elkashef, A., Munson, R.C., Gellad, F., 1993. Structural abnormalities in deficit and non-deficit schizophrenia. American Journal of Psychiatry 150, 59–65.

Cendes, F., Andermann, F., Gloor, P., Lopes-Cendes, I., Andermann, E., Melanson, D., Jones-Gotman, M., Robitaille, Y., Evans, A., Peters, T., 1993a. Atrophy of mesial structures in patients with temporal lobe epilepsy: cause or consequence of repeated seizures? Annals of Neurology 34, 795–801.

Cendes, F., Leroux, F., Melanson, D., Ethier, R., Evans, A., Peters, T., Andermann, F., 1993b. MRI of amygdala and hippocampus in temporal lobe epilepsy. Journal of Computer Assisted Tomography 17, 206–210.

Cuenod, C.A., Denys, A., Michot, J.L., Jehensen, P., Forette, F., Kaplan, D., Syrota, A., Boller, F., 1993. Amygdala atrophy in Alzheimer's disease: an in vivo magnetic resonance imaging study. Archives of Neurology 50, 941–945.

DeLisi, L.E., Dauphinais, I.D., Gershon, E.S., 1988. Perinatal complications and reduced size of brain limbic structures in familial schizophrenia. Schizophrenia Bulletin 14, 185–191.

Duvernoy, H.M., 1988. The Human Hippocampus: An Atlas of Applied Anatomy. J.F. Bergmann Verlag, München.

Filipek, P.A., Richelme, C., Kennedy, D.N., Caviness, V.S., 1994. The young adult human brain: an MRI-based morphometric analysis. Cerebral Cortex 4, 344–360.

Filipek, P.A., Semrud-Clikeman, M., Steingard, R.J., Renshaw, P.F., Kennedy, D.N., Biederman, J., 1997. Volumetric MRI analysis comparing subjects having attention-deficit hyperactivity disorder with normal control subjects. Neurology 48, 589–601.

Heckers, S., Heinsen, H., Heinsen, Y.C., Beckmann, H., 1990. Limbic structures and lateral ventricle in schizophrenia: a

quantitative postmortem study. Archives of General Psychiatry 47, 1016–1022.

Herzog, A.G., Kemper, T.L., 1980. Amygdaloid changes in aging and dementia. Archives of Neurology 37, 625–629.

Honeycutt, N.A., Smith, P.D., Aylward, E., Li, Q., Chan, M., Barta, P.E., Pearlson, G.D., 1998. Mesial temporal lobe measurements on magnetic resonance imaging scans. Psychiatry Research: Neuroimaging 83, 85–94.

Jack, C.R., Jr., Petersen, R.C., Xu, Y.C., Waring, S.C., O'Brien, P.C., Tangalos, E.G., Smith, G.E., Ivnik, R.J., Kokmen, E., 1997. Medial temporal atrophy on MRI in normal aging and very mild Alzheimer's disease. Neurology 49, 786–794.

Kate, W.R., Abrams, M.T., Kaufmann, W.E., Breiter, S.N., Reiss, A.L., 1997. Reliability and validity of MRI measurement of the amygdala and hippocampus in children with fragile X syndrome. Psychiatry Research: Neuroimaging 75, 31–48.

Krasuki, J.S., Alexander, G.E., Horwitz, B., Daly, E.M., Murphy, D.G.M., Rapoport, S.I., Schapiro, M.B., 1998. Volumes of medial temporal lobe structures in patients with Alzheimer's disease and mild cognitive impairment (and in healthy control subjects). Biological Psychiatry 43, 60–68.

Laakso, M.P., Partanen, K., Lehtovirta, M., Hallikainen, M., Hanninen, T., Vainio, P., Riekkinen, P., Sr., Soininen, H., 1995. MRI of amygdala fails to diagnose early Alzheimer's disease. NeuroReport 6, 2414–2418.

Lawrie, S.M., Abukmeil, S.S., 1998. Brain abnormality in schizophrenia: a systematic and quantitative review of volumetric magnetic resonance imaging studies. British Journal of Psychiatry 172, 110–120.

LeDoux, J.E., 1995. Emotion: clues from the brain. Annual Review of Psychology 46, 209–235.

Lehéricy, S., Baulac, M., Chiras, J., Pierot, L., Martin, N., Pillon, B., Deweer, B., Dubois, B., Marsault, C., 1994. Amygdalohippocampal MR volume measurements in the early stages of Alzheimer disease. American Journal of Neuroradiology 15, 929–937.

Mathalon, D.H., Sullivan, E.V., Rawles, J.M., Pfefferbaum, A., 1993. Correction for head size in brain-imaging measurements. Psychiatry Research: Neuroimaging 50, 121–139.

McGaugh, J.L., Cahill, L., 1997. Interaction of neuromodulatory systems in modulating memory storage. Behavioural Brain Research 83, 31–38.

Roberts, M., Hanaway, J., 1970. The Atlas of the Human Brain in Section. Lea and Febiger, Philadelphia.

Robins, L.N., Helzer, J., Croughan, J., Ratcliff, K., 1981. National Institutes of Mental Health Diagnostic Interview Schedule: its history, characteristics and validity. Archives of General Psychiatry 38, 38l–389.

Rosene, D.L., Van Hoesen, G.W., 1987. The hippocampal formation of the primate brain: a review of some comparative aspects of cytoarchitecture and connections. In: Jones, E.G., Peters, A. (Eds.), Cerebral Cortex. Plenum Press, New York, pp. 345–456.

Rossi, A., Stratta, P., Mancini, F., Gallucci, P.M., Mattei, P., Core, L., Di Michele, V., Casacchia, M., 1994. Magnetic resonance imaging findings of amygdala-anterior hippocampus shrinkage in male patients with Schizophrenia. Psychiatry Research 52, 43–53.

Scott, S.A., DeKosky, S.T., Scheff, S.W., 1991. Volumetric atrophy of the amygdala in Alzheimer's disease: quantitative serial reconstruction. Neurology 41, 351–356.

Sheline, Y.I., Gado, M.H., Price, J.L., 1998. Amygdala core nuclei volumes are decreased in recurrent major depression. Neuroreport 9, 2023–2028.

Shenton, M.E., Kikinis, R., Jolesz, F.A., Pollack, S.D., LeMay, M., Wible, C.G., Hokama, H., Martin, J., Metcalf, D., Coleman, M., McCarley, R.W., 1992. Abnormalities of the left temporal lobe and thought disorder in schizophrenia: a quantitative magnetic resonance imaging study. New England Journal of Medicine 327, 604–612.

Soininen, H.S., Partanen, K., Pitkanen, A., Vainio, P., Hanninen, T., Hallikainen, M., Koivisto, K., Riekkinen, P.J., 1994. Volumetric MRI analysis of the amygdala and the hippocampus in subjects with age-associated memory impairment: correlation to visual and verbal memory. Neurology 44, 1660–1668.

Tsuchiya, K., Kosaka, K., 1990. Neuropathological study of the amygdala in presenile Alzheimer's disease. Neurological Science 100, 165–173.

Tsui, W. T., 1995. Multimodal Image Data Analysis System (MIDAS), Version 1.0. (unpublished manual), N.Y. University School of Medicine, New York.

Watson, C., Andermann, F., Gloor, P., Jones-Gotman, M., Peters, T., Evans, A., Olivier, A., Melanson, D., Leroux, G., 1992. Anatomic basis of amygdaloid and hippocampal volume measurement by magnetic resonance imaging. Neurology 42, 1743–1750.

Watson, C., Jack, C.R., Cendes, F., 1997. Volumetric magnetic resonance imaging: clinical applications and contributions to the understanding of temporal lobe epilepsy. Archives of Neurology 54, 1521–1531.